This article has been accepted and will be published in the next available issue of this journal. Content is final, but pagination will differ.



# *In situ* calibration of light sensors for long-term monitoring of vegetation

Hongxiao Jin and Lars Eklundh

***Abstract*—Light sensors are increasingly used to monitor vegetation growing status by measuring reflectance or transmittance in multispectral or photosynthetically active radiation (PAR) bands. The measurements are then used to estimate vegetation indices or the fraction of absorbed PAR (FPAR) in a continuous and long-term manner, and to serve as inputs to environmental monitoring and calibration / validation data for satellite remote sensing. However, light-sensor calibration is often overlooked or not properly attended to, which leads to difficulties when comparing measurement results across sites and through time. In this paper we investigate a practical and accurate user-level *in situ* calibration method in daylight. Calibration of a sensor pair is made for measuring either bihemispherical reflectance (BHR) or hemispherical-conical reflectance (HCR), the two most common ground-based spectral measurements. Procedures and considerations are suggested for user calibration. We also provide a method for calibrating and measuring single-sensor reflectance-derived Normalized Difference Vegetation Index (NDVI) from red and near-infrared (NIR) bands. The calibration error propagation is analysed and the induced uncertainties in vegetation reflectance and NDVI are evaluated. The analysis and field measurements show that NDVI estimated from a user calibration factor can be as accurate as, or even more accurate than, manufacturer calibration. The *in situ* calibration described here remedies the situation that reflectance for large field-of-view sensors cannot always be estimated from manufacturer's calibration. The method developed in the paper may help improving the reliability of long-term field spectral measurements and contribute to the near-surface remote sensing of vegetation.**

***Index Terms*—Calibration, error propagation, fraction of absorbed photosynthetically active radiation (FPAR), light sensor, near-surface remote sensing, Normalized Difference Vegetation Index (NDVI), reflectance, uncertainty, vegetation monitoring.**

## I. Introduction

THIS paper deals with accurate *in situ* calibration of field-mounted light sensors for generating reliable long-term data of vegetation properties. Measurement of radiation has been instrumental in understanding light interception and photosynthetic light use in vegetation canopies (e.g. [1]) and canopy growing status (e.g. [2]). More recently, ground-based spectral measurements of vegetation has become increasingly used [3-6], since spectral data carry detailed information about vegetation properties. Long-term spectral measurements provide reference data for evaluating satellite-derived biophysical parameters [7], phenology [8], complement ground carbon flux observations [9], and improve understanding of vegetation growing dynamics [6],[10] and disturbance impact [11],[12]. Spectral measurements are usually carried out from towers or masts using instruments measuring a few selected bands in red, near-infrared (NIR), photosynthetically active radiation (PAR, wavelength 400-700 nm), and other narrow bands, owing to the low instrument cost, easy maintenance, and straightforward data results [5],[10]. However, ground measurements from uncalibrated light sensors (either laboratory calibration or field cross-calibration) have very limited use, and data from long-term sensor measurements without regular calibration are unconvincing.

Usually light-sensor calibration is made by sensor manufacturers or professional laboratories. This type of calibration is time-consuming, expensive, and disrupts measurements since sensors have to be dismounted and gathered from field sites, and delivered back and forth. Moreover, laboratory calibration of large field-of-view (FOV) sensors in radiometric quantities is difficult, and some sensor manufacturers do not provide such radiometric calibration. Instead they provide the relative sensitivity between red and NIR channels of a sensor to only enable computing a Normalized Difference Vegetation Index (NDVI). Reflectance cannot be measured with such sensor calibration, and therefore it is not possible to compute non-ratio-based vegetation index, such as GEMI [13], EVI [14], and PPI [15], which have several good properties for vegetation monitoring.

Alternative calibration methods have been explored, e.g. calibration of NDVI sensors against a spectroradiometer in daylight to enable absolute radiometric quantity measurements [6],[16]. However, a precision spectroradiometer is a delicate and costly instrument and this is not an optimal user-level calibration method. Moreover, it is not appropriate to calibrate a conical-FOV sensor by pointing it towards the sky with variable fractions of direct and diffuse illumination and no guarantee of a 100% diffuse light required in such calibrations. Pontailler and Genty [17] reported on a simple

Manuscript received November 05, 2013; revised June 10, 2014 and September 17, 2014; accepted November 17, 2014. This work was supported by a grant from the Faculty of Science of Lund University (PI: Lars Eklundh).

H. Jin and L. Eklundh are with the Department of Physical Geography and Ecosystem Science, Lund University, Sölvegatan 12, 22362, Lund, Sweden (e-mail: hongxiao.jin@nateko.lu.se; lars.eklundh@nateko.lu.se).

Color versions of one or more of the figures in this paper are available online at http://ieeexplore.ieee.org.

Digital Object Identifier 10.1109/TGRS.2014.2375381.

calibration method for hemispherical red and NIR sensors by pointing them towards the sun or a halogen lamp which was assumed to have a constant red:NIR ratio. However, the ratio may vary with the sensor spectral response function, and the authors did not show how to use this simple calibration for either reflectance or NDVI estimation. Gamon *et al.* [11] calibrated a dual-detector spectrometer against a diffuse white reflectance reference panel to obtain a cross-calibration factor for rectifying the "raw" reflectance measured by a tram system. However, they noticed in their measurements that the calibration factors are dependent on sky conditions. Variation of calibration factors with sky conditions was confirmed by Garrity *et al.* [18], and they suggested calibrations across a range of sky conditions and to use the proper one for the corresponding condition. Ryu *et al.* [19] did cross-calibration for their home-made NDVI sensor pairs against a low-cost spectrometer, and directly corrected the sensor-pair-measured reflectance by a factor obtained from the comparison with spectrometer-measured reflectance. However, such inter-comparison experiment needs careful design [20], otherwise it might be problematic considering different sensor-viewing geometries and spectral bandwidths over possibly non-identical vegetation targets. The widely scattered data in Ryu *et al.* [19, Fig. 4] comparison plots showed that this method may be not precise enough for calibration purposes.

It is possible to define an accurate and simple *in situ* calibration method based on relative sensitivities. In this paper we propose that the user-level *in situ* calibration of light sensors in daylight based on relative sensitivities is as accurate as, or even more accurate than, the calibration in laboratory by the manufacturer. We explain the theory and investigate the accuracy of the method by field measurements and by analyzing the calibration error propagation. Our results demonstrate that a simple calibration protocol can lead to accurate measurements of spectral reflectance and vegetation indices such as the NDVI, suitable for long-term monitoring of vegetation conditions. The method is also suitable for calibrating PAR sensors for fraction of absorbed PAR (FPAR) measurement. We also discuss the calibration and use of a *single sensor* for estimating "reflectance-derived" NDVI. The single-sensor method has been used by researchers to estimate "radiance-derived" NDVI (e.g. [6]), and has proven advantageous for eliminating uncertainties from the upward-looking sensor. Our calibration method will give reflectance-derived NDVI, even though reflectance cannot be estimated from a single downward-looking sensor. We demonstrate examples of field measurements from both sensor-pair and single-sensor methods, and show how these methods confirm each other in NDVI estimation.

## II. Measurement of Vegetation Reflectance of Light

Reflectance is the ratio of reflected to incident radiant flux [21]. Usually, two kinds of reflectance are measured with sensor pairs from ground spectral sampling towers [5] (Fig.1): bihemispherical reflectance (BHR) and hemispherical-conical reflectance (HCR). Both quantities require downwelling irradiance measurement using an upward-looking sensor with a cosine diffuser that enables a hemispherical view, whereas the upwelling reflected flux is measured in different ways: by a downward-looking hemispherical-view sensor in BHR and a conical field-of-view (FOV) sensor in HCR.

For deriving calibration theory we need to present the principles of light reflectance measurement. The sensor has a photo-sensitivity $S$, giving a reading $V$ (dark measurement drift corrected, the same hereinafter) in voltage. So, the sensor measured light flux density $E$ (radiometric unit: $W \cdot m^{-2}$, for conversion to quantum light unit $\mu mol \cdot m^{-2} \cdot s^{-1}$ see [22]) is

$$E = S \cdot V + \varepsilon, \quad (1)$$

where ε is a small noise term of the measurement (the systematic error of dark current being excluded). Assume a sensor pair (Sensor 1 and 2) is used to measure downwelling irradiance $E_1$ and upwelling reflected flux density $E_2$. The equation group for ground-based spectral measurement configuration (Fig. 1) is

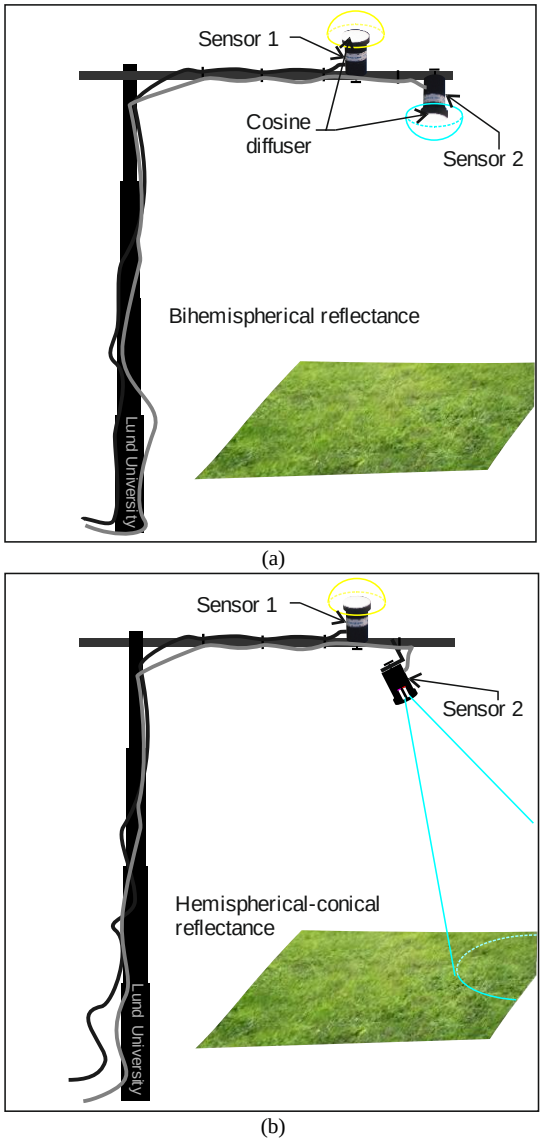


Fig. 1. Configurations of ground-based spectral measurement for vegetation monitoring by a pair of light sensors. (a) Both sensors have a cosine diffuser and measure bihemispherical reflectance. (b) The downward-looking sensor has a conical-FOV and measures hemispherical-conical reflectance together with the upward-looking hemispherical sensor.

$$\begin{cases} E_1 = S_1 \cdot V_1 + \varepsilon_1 \\ E_2 = S_2 \cdot V_2 + \varepsilon_2 \end{cases}. \quad (2)$$

The reflectance $R$ of the sensor footprint area A is:

$$R = \frac{A \cdot E_2}{A \cdot E_1} = \frac{S_2 V_{2obs} + \varepsilon_2}{S_1 V_{1obs} + \varepsilon_1} \approx \frac{1}{k} \cdot \frac{V_{2obs}}{V_{1obs}} + \varepsilon, \quad (3)$$

where $k$=$S_1$/$S_2$, the ratio of the two sensor sensitivities, and ε is the total small noise term inherited from the two sensor readings.

We assume that the conical-FOV sensor has undergone calibration against a radiance standard and measures flux density per solid angle, i.e. a radiance quantity. In order to compute reflectance, the value of projected hemispherical solid angle π (unit: sr) should be multiplied with the radiance value to get flux density quantity $E_2$ so that the HCR is unitless. We assume the factor π is implicitly included in the sensitivity $S_2$ and thus the sensor measures flux density in Fig. 1(b). Therefore (3) suits both BHR and HCR.

The sensor-pair calibration is to estimate the sensitivity ratio $k$ of the two sensors, and then vegetation reflectance can be computed by plugging $k$ in (3) and ignoring the noise term $\varepsilon$. From multispectral reflectance, various vegetation indices can then be estimated. The same approach is also suitable for PAR sensors to estimate PAR reflectance and transmittance of the vegetation canopy, and subsequently to estimate FPAR.

## III. Sensor-Pair Calibration

In this section we describe a user-level cross-calibration method of a sensor pair in daylight for estimation of BHR or HCR (Fig. 2), suitable for multispectral and PAR sensors. Calibration into absolute radiometric units is often not necessary, since users are usually only interested in measuring light reflectance or transmittance of plant canopies, which are based on ratio factors. Thus, it is sufficient to calibrate the relative sensitivities of a sensor pair for accurately estimating light reflectance or transmittance.

Suppose a light sensor with an ideal angular response is oriented upwards measuring incoming solar radiation. The incident radiant flux density $E_0$ with a sun zenith angle $\theta$ and an azimuth angle $\phi$ has a diffuse fraction $d_c$ and a direct fraction 1 - $d_c$. The light sensing surface of the sensor has a slight tilt angle $\theta'$ from the horizontal, towards an azimuthal direction $\phi'$. By neglecting the nearby ground reflection, the sensor measured light flux density is [23]

$$E = E_0 \cdot [d_c + (1 - d_c) \cdot \cos(\alpha)], \quad (4)$$

where α is the angle of incidence of direct light beam to the sensor, and

$$\cos(\alpha) = \cos(\theta) \cdot \cos(\theta') + \sin(\theta) \cdot \sin(\theta') \cdot \cos(\phi - \phi'). \quad (5)$$

The sensor pair being cross-calibrated measures the same irradiance quantity $E$ and the sensor readings also follow (2) by considering both $E_1$ and $E_2$ as downwelling radiation. Two situations are discussed here: the sensors having identical or non-identical view.

### A. Identical sensor view $E_1 = E_2$

If both sensors are exactly level, or in identical positions, $\alpha_1 = \alpha_2$, then $E_1 = E_2$ by (4). The two quantities will also be equal if $d_c$ = 1, a 100% diffuse daylight. It can be shown from (2) that the two sensor readings $V_1$ and $V_2$ will have a linear relationship:

$$V_2 = \frac{S_1}{S_2} \cdot V_1 + \frac{\varepsilon_1 - \varepsilon_2}{S_2} = k \cdot V_1 + b, \quad (6)$$

where, $k = S_1 / S_2$, and $b = (\varepsilon_1 - \varepsilon_2) / S_2$, can be accurately estimated from calibration measurements of the two upward-looking sensors.

For a downward-looking conical-FOV sensor, a white reference panel is placed horizontally in the sensor nadir direction, which may be viewed together as an upward-looking sensor system and measuring irradiance $E$ [Fig. 2(b)]. The white reference panel should be routinely calibrated to give a reflectance factor $R_L$ (wavelength-dependent). For a


(a)

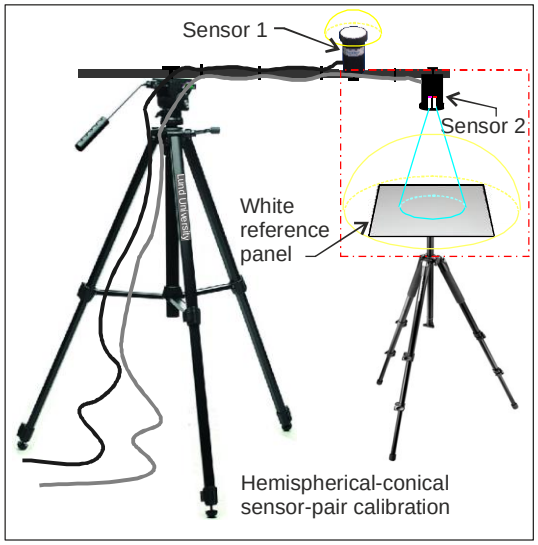


(b)

Fig. 2. Configurations of sensor-pair calibration. (a) Bemispherical sensor pair. Both sensor measure the same irradiance quantity. (b) Hemispherical-conical sensor pair. The downward-looking conical-FOV senor (Sensor 2) and the white reference panel together are viewed as a sensor system measuring irradiance quantity, assumed to be equal to the irradiance measured by the hemispherical view sensor (Sensor 1).

99% white panel the value is around 0.99 and results in an underestimate in $V_2$ of Sensor 2 and consequently an underestimated $k$ in (6). Therefore, the reading $V_2$ should be rectified by a factor of 1 / $R_L$, when estimating the factors $k$ and $b$. Otherwise the simply modified (3)

$$R = \frac{R_L}{k} \cdot \frac{V_{2obs}}{V_{1obs}}, \tag{7}$$

is used to calculate reflectance.

### B. Non-identical sensor view $E_1 \neq E_2$

In a real situation, it is hardly 100% diffuse daylight, nor are the surfaces exactly level, and then $E_1 \neq E_2$. Plug (4) in (2) to get

$$\frac{d_c + (1-d_c)\cdot\cos(\alpha_1)}{d_c + (1-d_c)\cdot\cos(\alpha_2)} = \frac{S_1 \cdot V_1 + \varepsilon_1}{S_2 \cdot V_2 + \varepsilon_2}. \tag{8}$$

After rearrangement,

$$\begin{aligned} V_2 = {} & \frac{d_c + (1-d_c)\cdot\cos(\alpha_2)}{d_c + (1-d_c)\cdot\cos(\alpha_1)} \cdot \frac{S_1}{S_2} \cdot V_1 \\ & + \frac{d_c + (1-d_c)\cdot\cos(\alpha_2)}{d_c + (1-d_c)\cdot\cos(\alpha_1)} \cdot \frac{1}{S_2} \cdot \varepsilon_1 - \frac{1}{S_2} \cdot \varepsilon_2 \end{aligned}. \tag{9}$$

The slope $k = \frac{d_c + (1-d_c)\cdot\cos(\alpha_2)}{d_c + (1-d_c)\cdot\cos(\alpha_1)} \cdot \frac{S_1}{S_2}$ of the $V_2$~$V_1$ line varies with the tilt of light sensing surfaces, diffuse fraction, and the solar zenith angle.

## IV. Single-sensor calibration for NDVI measurement

Reflectance cannot be measured by a single sensor with red and NIR channels, but the reflectance-derived NDVI can still be computed. Here we describe a method by using the user-level calibration of a single sensor (with conical-FOV) against a horizontally placed white reference panel in the sensor nadir direction in daylight. The only assumption is that the solar spectral red:NIR ratio is constant [17]. To reduce the uncertainty from red:NIR ratio variation, the calibration and vegetation measurement should be made under cloudless sky and also avoiding large sun zenith angle.

Similarly as (2), we write down an equation group for red and NIR channels for the calibration data, while considering the reflectance factor $R_{L\_red}$ in red and $R_{L\_NIR}$ in NIR of the white reference panel:

$$\begin{cases} E_{red} \cdot R_{L\_red} = S_{red} \cdot V_{red} + \varepsilon_{red} \\ E_{NIR} \cdot R_{L\_NIR} = S_{NIR} \cdot V_{NIR} + \varepsilon_{NIR} \end{cases}. \tag{10}$$

After rearrangement we get:

$$V_{NIR} = k_s \cdot V_{red} + b_s, \tag{11}$$

where

$$k_s = \frac{1}{k_L} \cdot \frac{E_{NIR}}{E_{red}} \cdot \frac{S_{red}}{S_{NIR}}, \quad \text{and} \quad b_s \approx (\frac{1}{k_L} \cdot \frac{E_{NIR}}{E_{red}} \cdot \varepsilon_{red} - \varepsilon_{NIR}) / S_{NIR}.$$

Here $k_L = \frac{R_{L\_red}}{R_{L\_NIR}}$ is the red:NIR ratio of the reflectance factor of the white reference panel that can be obtained from the per-wavelength calibration of the panel, and $k_L \approx 1$ for a white reference panel that has a flat response across visible and NIR spectra. There will be a linear relationship between $V_{NIR}$ and $V_{red}$ given a constant ratio $E_{NIR}$ / $E_{red}$ of the incoming radiation. The slope $k_s$ can be estimated by linear fitting of the calibration data, and then used to estimate NDVI.

During vegetation observations, the sensor equation is written as:

$$\begin{cases} E_{red\_obs} \cdot R_{red} = S_{red} \cdot V_{red\_obs} \\ E_{NIR\_obs} \cdot R_{NIR} = S_{NIR} \cdot V_{NIR\_obs} \end{cases}, \tag{12}$$

where $R_{red}$ and $R_{NIR}$ are vegetation reflectance in red and NIR bands respectively. $E_{red\_obs}$ and $E_{NIR\_obs}$ are incident red and NIR flux density during vegetation observation. The small noise term ε is neglected to facilitate the further derivation. Reorganizing (12) we can write a ratio vegetation index (RVI):

$$RVI = \frac{R_{NIR}}{R_{red}} = \frac{E_{red\_obs}}{E_{NIR\_obs}} \cdot \frac{S_{NIR}}{S_{red}} \cdot \frac{V_{NIR\_obs}}{V_{red\_obs}}. \tag{13}$$

Since we assume a constant red:NIR ratio, $E_{red\_obs} / E_{NIR\_obs} = E_{red} / E_{NIR}$. Checking the slope term $k_s$ in (11), we find

$$RVI = \frac{1}{k_s \cdot k_L} \cdot \frac{V_{NIR\_obs}}{V_{red\_obs}}. \tag{14}$$

The NDVI can thus be estimated from RVI:

$$NDVI = (RVI - 1)/(RVI + 1). \tag{15}$$

## V. Calibration error propagation and uncertainty evaluation

The uncertainty of a calibration method should be evaluated in conformity with international standards [24],[25], to justify if the calibration result is accurate enough to meet the requirement of a specific measurement, and possibly reduce calibration uncertainties to meet the requirement. We here derive calibration error propagation equations to evaluate the consequent uncertainties in vegetation reflectance and NDVI estimation. We compare the reflectance uncertainty resulted from user *in situ* calibration with that from manufacturer laboratory calibration. The relative standard uncertainty [25] is used here, and it is assumed that the uncertainty components are independent of each other.

### A. Reflectance uncertainties

*1)* From *manufacturer calibration*

Given Sensor 1 measuring downwelling irradiance and Sensor 2 upwelling reflected flux density, the reflectance is computed from (3) by ignoring the noise term. The standard uncertainty $u$(R) in measured reflectance R (relative value $u$(R)/R, the same hereinafter) resulting from the uncertainty in sensitivity calibrations can be expressed as [25],[26]:

$$\frac{u(R)}{R} = \sqrt{\left[\frac{\partial \ln R}{\partial S_1} \cdot u(S_1)\right]^2 + \left[\frac{\partial \ln R}{\partial S_2} \cdot u(S_2)\right]^2} = \sqrt{\left[\frac{u(S_1)}{S_1}\right]^2 + \left[\frac{u(S_2)}{S_2}\right]^2}. \tag{17}$$

*2) From* user *calibration*

From (3), it can be deduced that:

$$\frac{u(R)}{R} = \sqrt{\left[\frac{\partial \ln R}{\partial k} \cdot u(k)\right]^2} \approx \frac{u(k)}{k}, \tag{18}$$

where the small noise term ε is omitted in the approximation.

### B. NDVI Uncertainties

*1) Sensor-pair method*

The standard uncertainty of NDVI inherited from the

uncertainty of reflectance measurements is

$$\frac{u(NDVI)}{NDVI}=\frac{1-NDVI^2}{2NDVI}\cdot\sqrt{\left[\frac{u(R_{NIR})}{R_{NIR}}\right]^2+\left[\frac{u(R_{red})}{R_{red}}\right]^2}. \quad (19)$$

Therefore the NDVI uncertainty depends on the NDVI level.

*2) Single-sensor method*

From the NDVI-RVI relation, it can be shown that the NDVI uncertainty inherited from RVI is:

$$\frac{u(NDVI)}{NDVI}=\frac{1-NDVI^2}{2NDVI}\cdot\frac{u(RVI)}{RVI}. \quad (20)$$

From (14), we have $u(RVI)/RVI=u(k_s)/k_s$, suggesting the measured RVI has the same standard uncertainty as $k_s$ from calibration. From (20) we see that the NDVI uncertainty in single-sensor method inherited from the calibration depends on the NDVI level, the same as sensor-pair method.

The error propagation equations of sensor-pair method also suit to evaluate uncertainties in PAR reflectance and transmittance, and in turn to evaluate FPAR uncertainty inherited from calibration errors.

## VI. Materials and Methods

### A. Sensors and materials

We have so far calibrated more than 30 pairs of NDVI sensors (SKR-series, expanded uncertainty ±5%, originally calibrated by the manufacturer, Skye Instruments Ltd, UK) with conical-FOV (25° or 60°) or hemispherical view, and PAR sensors (JYP-1000, SDEC France) on the office building roof or in the open field using either Minicube VV (accuracy 0.01%, EMS Brno, Czech Republic) or CR1000 (accuracy ±0.06%, Campbell Scientific, Inc. USA) data loggers. A 99% reflective Spectralon white reference panel (model SRT-99-120, calibrated, expanded uncertainty 0.006, Labsphere Inc., USA) was used for calibrating conical-FOV sensors up to 60°. Typical directional responses of these sensors and the white reference panel are shown in Fig. 3. Most of the sensors are currently used at spectral sampling network sites across the Arctic region [9], the Nordic region [10], and the African Sahel.

### B. Calibration procedures

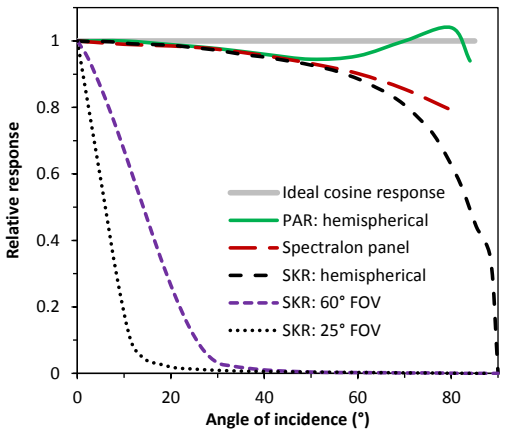


Fig. 3. Typical directional response of the sensors and Spectralon panel used in the test (modified from [27]). Curves are relative to the response at 0° incident angle and normalized against cosine response at each incident angle.

The following procedures were followed in our calibration measurement.

1) Estimate the whole system zero drift in dark conditions. Such a test is done in a dark room or by covering the sensors with thick spectrally black cloth.
2) Connect the sensor pair to the adjacent channels of a data logger, with a sampling interval of no longer than 5 seconds. Data are saved without post-averaging.
3) Ensure that the light sensing surfaces are level, including the cosine diffuser and white reference panel; check with a high sensitive (better than 0.5°) and accurate circular level. No highly reflective materials are in the vicinity of the light sensing surfaces and no shadow should cast on the surfaces.
4) When calibrating a conical-FOV sensor, the sensor is oriented nadir-viewing, as far away as possible above the levelled reference panel in the sensor nadir direction. Meanwhile the sensor viewing area must fall totally within the panel.
5) The calibration of a sensor pair is carried out preferably under overcast sky with a wide range of daylight illumination, for at least 20 minutes. If the measurement is made under clear sky, the calibration should last at least one hour before and one hour after local solar noon time, in order to check if the regression lines before and after solar noon are consistent.
6) For the single-sensor method, the sensor is calibrated under cloudless sky at around solar noon.
7) Once the calibration data are collected, check the data with time series curves or scatter plots. Spurious data points due to rapidly changing cloud cover or other reasons should be removed.
8) Estimate the slope of (6) for a sensor pair, or (11) for a single sensor using linear regression.
9) Redo calibration and dark measurement if the intercept $b$ is larger than 5% of the $k{\cdot}V_1$ term, or regression lines before and after solar soon are not consistent. Particularly check if the light sensing surfaces are level or not.

### C. Calibration experiments

The user-level calibration techniques and procedures have been tested under overcast and cloudless sky, mornings and afternoons, by different operators and dataloggers. The following four experiments were made on the Lund University INES Department building roof (55.71°N 13.20°E).

1) Repeat tests on an SKR-series NDVI sensor pair (#42084—25° FOV vs. #42085—hemispherical view) were done using a Minicube VV datalogger from 8:50 to 16:10 on Sep. 11, 2013, a day with frequently changing cloud cover, to test the dependency of calibration factor on illumination conditions. Eight sets of 20 minutes data (10 minutes before and after the hour) of 5 seconds sampling interval in red and NIR channels were extracted for linear fitting analysis separately. The incoming PAR was simultaneously recorded to monitor how illumination varied.

2) A comparison experiment was made by two operators separately using two dataloggers (Minicube VV vs. CR1000) both on two pairs of newly manufacturer-calibrated SKR-series bihemispherical NDVI sensors (Pair 1 #33445 vs. #33444, Pair 2 #33451 vs. #33450), to test if the user-level

calibration factor is consistent with that from manufacturer calibration and independent of operators and dataloggers. The experiment was made in two days: from 12:00 to 14:00 on Sep 3, 2013 (cloudless sky) using CR1000 and from 11:30 to 15:30 on Sep 4, 2013 (overcast sky) using Minicube VV.

3) The experiment on single-sensor calibration was conducted on #42084 NDVI sensor with a white reference panel from 16:00 to 18:00 on Sep 4, 2013 (overcast sky) and from 9:00 to 15:20 on Sep 6, 2013 (cloudless sky) respectively, to test how the single-sensor calibration slope $k_s$ depends on daylight conditions, particularly the red:NIR ratio of daylight illumination. A hemispherical view senor (#42085) with red and NIR channels was used to monitor the red:NIR ratio of sky radiation.

4) The last experiment was done to test tilt surface influences by studying the scatter plot of the sensor-pair calibration dataset with one surface tilt and the other not. The experiment was made on a sensor pair under cloudless sky from 9:00 to 15:20 on Sep.6, 2013. The measurements of #42084 sensor against a horizontally placed white reference panel were reused. The other sensor (#33451, hemispherical view) was looking upwards with ca. 2° eastward tilt from the horizontal.

### D. Numerical simulations

#### 1) Simulation of tilt surface influence

In order to further understand how a slight tilt influences the sensor-pair calibration and provide suggestions, a numerical simulation was done using (4) with $d_c = 0$ and $E_0 = 110$ units to compute readings of a sensor pair. One sensor of the pair tilted eastward 1° from the horizontal, and the other was level. The sun positions were computed with a high accuracy (±0.0003°) algorithm [28] for 55.71°N, 13.20°E from 9:00 to 15:20 on Sep.6, 2013, the same location and time as in the tilt experiment to facilitate comparison.

If the light sensing surface is tilt, all three factors—tilt angle, diffuse fraction, and sun zenith angle—affect the calibration slope $k$ in (9). By comparing (6) and (9), the relative error of slope $k$ in relation with these three factors were simulated as

$$\frac{\Delta k}{k} = \frac{d_c + (1-d_c)\cdot\cos(\alpha_2)}{d_c + (1-d_c)\cdot\cos(\alpha_1)} - 1. \quad (21)$$

Since there are two light sensing surfaces for sensor-pair calibration and both may tilt, we assumed the same tilt angle for both surfaces but in opposite directions in the illumination principal plane, the worst case generating the largest calibration error in slope $k$ for a given tilt angle. The simulation was exemplified with tilt angles from 0 to 1° and daylight diffuse factions from 0 to 1 for solar zenith angles of 20°, 40° and 60°, in order to provide suggestions for *in situ* calibrations in late spring or early summer at our field sites in the African Sahel, the Nordic region, and the Arctic region.

#### 2) Simulation of calibration errors for NDVI uncertainty evaluation

Uncertainties in NDVI due to calibration errors were evaluated with (19) for sensor-pair and (20) for single-sensor methods respectively. The NDVI uncertainties from both methods rely on uncertainties in the slope $k$ in the linear regression. The combined standard uncertainty [25] in the slope $k$ can be estimated as

$$\frac{u_c(k)}{k} = \sqrt{\sum_i (u_i)^2}, \quad (22)$$

where $u_i$ are relative uncertainties in terms of slope $k$ from difference sources (assumed to be uncorrelated), such as errors due to surface tilting, uncertainty in the reflectance factor $R_L$ of the white reference panel if involved, datalogger accuracy, errors in repeat tests and so on.

The user calibration uncertainty was compared with that from manufacturer calibration in laboratory. The manufacturer calibration (expanded) uncertainty in sensitivity of SKR-series sensors is claimed to be ±5% at a confidence level of 95%, thus a standard uncertainty ±2.5% was used to evaluate uncertainties in reflectance and NDVI.

For the single-sensor method, besides the measurement error in the calibration factor, the assumption of a constant red:NIR ratio in daylight illumination may lead to a certain error in the factor, considering the potential difference of the ratio between calibration daylight and vegetation measurement daylight. We used relative standard errors (1% and 10% respectively) in red:NIR ratio to quantify the relative error in the factor $k$ for NDVI measurement.

### E. Field NDVI measurements

We carried out regular *in situ* calibrations for the spectral sampling network sites. An example of using such calibrations to estimate NDVI over the Fäjemyr bog, S. Sweden in 2012-2013 is presented here. At this site, a pair of SKR-1800 NDVI sensors (central wavelengths 650nm and 860 nm, bandwidth 50nm) was mounted on a 10-meter telescopic mast, measuring NDVI of a peat bog. The downward-looking sensor has a 60° FOV and measures radiance from the vegetation, and the upward-looking sensor has an acrylic cosine diffuser and measures irradiance. When calibrating the sensor pair, the sensors were dismounted from the mast and fixed on a tripod at the site. The aforementioned calibration procedures were carefully followed during the calibration measurements. Once the calibration was finished, the sensors were immediately mounted back on to the mast and the vegetation monitoring was continued. The regression slope $k$ from the calibration dataset was estimated and then used to compute NDVI time series. Meanwhile we computed $k_s$ from the calibration dataset of the 60°-FOV sensor to compute single-sensor derived NDVI. We also used the manufacturer calibration parameters (estimated in 2009) to compute NDVI for comparison.

## VII. Results

### A. Calibration experiments

#### 1) Repeat tests under variable illumination

The scatter plots of the eight sets of repeat tests are shown in Fig. 4(a) and (b), together with the simultaneous PAR time series in Fig. 4(c). The linear regression results for the scatter plots are given in Table I. The figure and table show that the user calibration had very good linearity in regression ($R^2$ > 0.99), and was seemingly independent of the rapidly changing illumination during the measurement. The residuals of eight sets of data using the mean fitting line also demonstrated independency of measurement time (i.e. sun zenith angle) and variations in illumination (not shown), except slightly larger residuals appearing for data points with frequent sudden

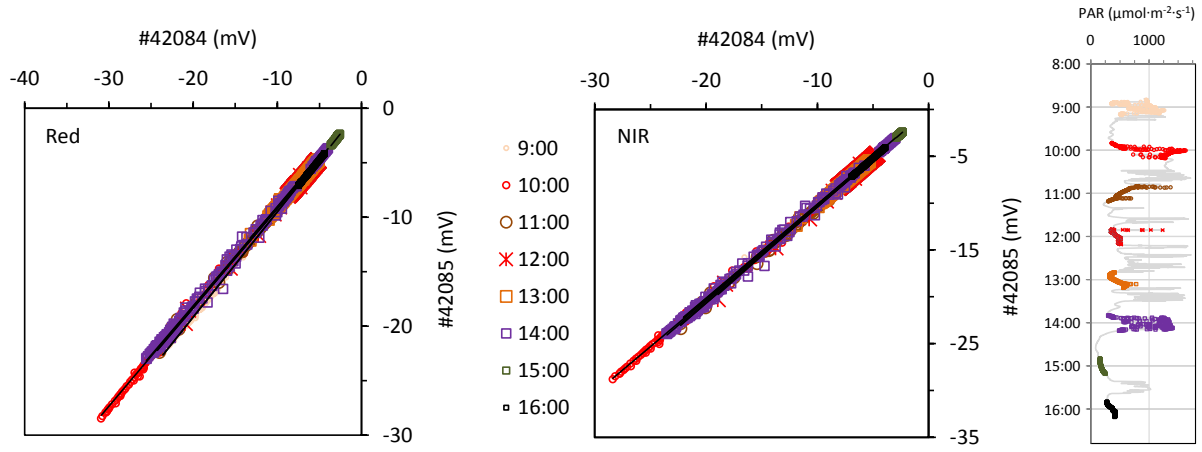


Fig. 4. Scatter plots in (a) red and (b) NIR of an NDVI sensor pair during eight sets of repeat test from 8:50 to 16:10 on Sep. 11, 2013. (c) Simultaneously measured PAR time series, indicating rapidly changing illumination conditions during the measurements.

TABLE I
SLOPE AND INTERCEPT OF THE LINEAR FITS IN EIGHT REPEAT TESTS

| Time | Red | | | NIR | | |
|---|---|---|---|---|---|---|
| | *k* | *b* | $R^2$ | *k* | *b* | $R^2$ |
| 9:00 | 0.970 | 0.204 | 0.998 | 1.003 | -0.118 | 0.999 |
| 10:00 | 0.917 | 0.155 | 0.999 | 1.000 | -0.322 | 0.999 |
| 11:00 | 0.925 | 0.047 | 0.999 | 1.029 | -0.148 | 0.999 |
| 12:00 | 0.908 | -0.130 | 0.998 | 1.046 | 0.078 | 0.998 |
| 13:00 | 0.885 | -0.222 | 0.999 | 1.024 | -0.067 | 1.000 |
| 14:00 | 0.903 | -0.095 | 0.998 | 1.023 | -0.006 | 0.999 |
| 15:00 | 0.973 | 0.100 | 0.999 | 1.039 | 0.001 | 1.000 |
| 16:00 | 0.943 | -0.004 | 1.000 | 1.034 | -0.031 | 1.000 |
| Mean | 0.928 | | | 1.025 | | |
| Std. of the M. [a] | 0.011 | | | 0.006 | | |
| Std. un. [b] | 1.2% | | | 0.6% | | |

[a] standard deviation of the mean.
[b] relative standard uncertainty: the ratio of standard deviation of the mean to the mean.

TABLE II
COMPARISON OF THE FACTOR *k* FROM USER CALIBRATION WITH THOSE GIVEN BY SENSOR MANUFACTURER.

| Sensor pair | Channel | Manufacturer factor [a] | User Calibration with MiniCube VV | | User calibration with CR1000 | |
|---|---|---|---|---|---|---|
| | | | Factor | Relative error vs. Manufacturer | Factor | Relative error vs. Manufacturer |
| #33445 vs. #33444 | Red | 1.068 | 1.064 | -0.37% | 1.055 | -1.22% |
| | NIR | 1.065 | 1.063 | -0.19% | 1.057 | -0.75% |
| #33451 vs. #33450 | Red | 0.970 | 0.991 | 2.16% | 1.016 | 4.74% |
| | NIR | 1.015 | 1.021 | 0.59% | 1.044 | 2.86% |

[a] Note: the factor *k* is the ratio of two sensitivities from the manufacturer calibration certificate.

illumination changes at 14:00. The relative standard uncertainty (the standard deviation of the mean divided by the mean [25]) in slope *k* was 1.2% for the red channel and 0.6% for the NIR channel for the tested sensor pair.

*2) Comparison with manufacturer calibration*

The test results are compared in Table II. The table shows that the relative errors of the user calibration vs. the manufacturer calibration were from -0.37% to 2.16% by one operator with MiniCube VV, and -1.22% to 4.74% by another operator with CR1000. Since the factor *k* from the manufacturer calibration has a combined standard uncertainty of ±3.54%, which can be estimated with (17) and (18) with a sensitivity uncertainty of ±2.5% specified by the manufacturer, the user calibration errors were within the combined expended uncertainty range of ±7.08%, and we cannot conclude an operator- or datalogger-dependency of the user-level calibration at a confidence level of 95%.

*3) Single-sensor calibration experiment*

The results of single-sensor slope $k_s$ in red and NIR channels tested under cloudless and overcast sky are shown in Fig. 5(a). The measurements under cloudless sky were split into two subsets: before and after solar noon. The scatter plots of the two subsets show an almost overlapped straight line, with a relative error of 0.3% in the regression slopes. However, the slope measured under overcast sky differed 13.2% from the cloudless sky measurement. The simultaneously measured red:NIR ratios [Fig. 5(b)] were relatively stable in cloudless sky during the measurement (before noon: 1.56 ± 0.01, after noon: 1.55 ± 0.01), and higher than the ratio measured under overcast sky (1.42 ± 0.03) by 9.5%. Such red:NIR ratio difference results in most of the large difference in slope $k_s$ between cloudless and overcast sky. Therefore, the single-sensor method may have limited use, for example the calibration under cloudless sky mainly being suitable for vegetation monitoring in clear days [6].

## B. *Influence of tilt surface*

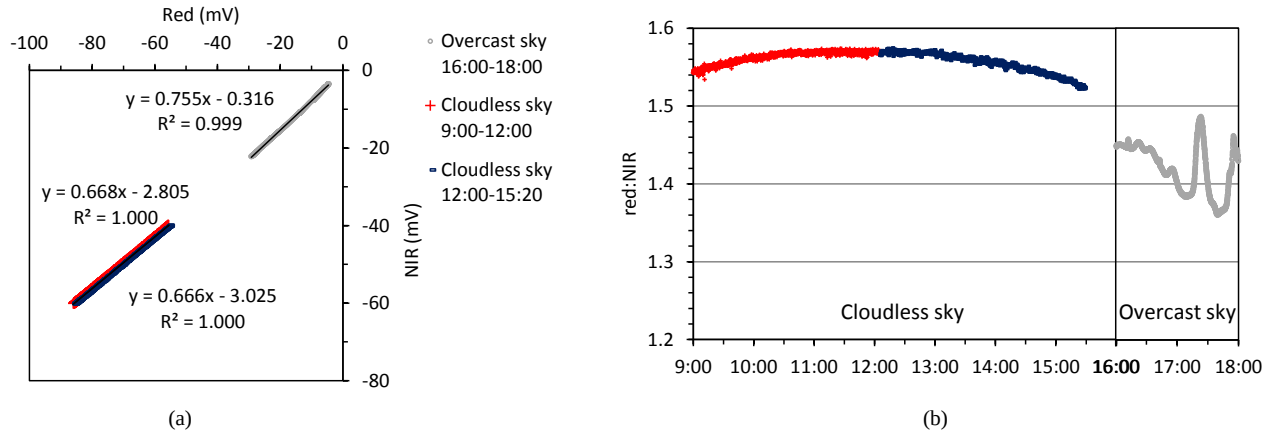


Fig. 5. (a) Single-sensor calibration experiments in dayligts on #42084 NDVI sensor with 25° FOV under cloudless sky (Sep 6, 2013) and overcast sky (Sep 4, 2013) respectively. (b) The red:NIR ratio of daylight illumination simultaneously measured by #42085 hemispherical view sensor with red and NIR channels.

The experiment results are exemplified with a red channel in Fig. 6(a), showing a large difference (14%) between the morning slope (1.165) and the afternoon slope (0.999) of their fitted lines. A similar difference was also seen in the NIR channel (not shown). A numerical simulation in Fig. 6(b) shows that the morning slope (1.070) and afternoon slope (0.939) differ 13% for 1.0° tilt. If decreasing the tilt angle from 1.0° to 0.5°, the difference of the slopes decreases to 6% ($k$=1.034 for morning and 0.969 for afternoon). The experiment and simulation suggest that calibration in clear days should be done both before and after solar noon so that the non-level surface, if any, can be identified and rectified. Such errors may be unnoticed without comparing both datasets before and after 12:00.

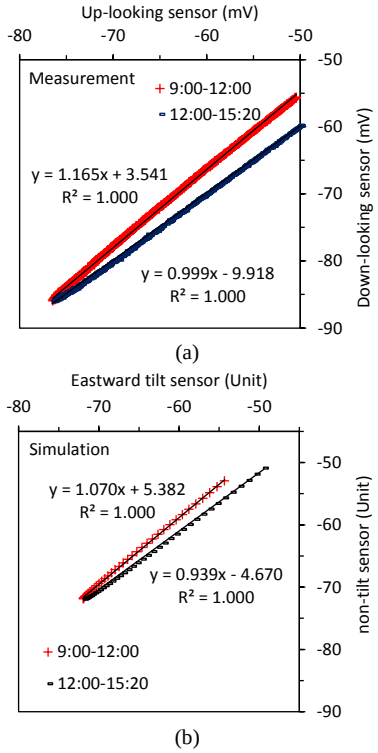


Fig. 6. (a) Calibration readings in red channel of a sensor pair. The upward-looking sensor had a cosine diffuser, tilting ca. 2° eastwards. The downward-looking sensor has 25° FOV, viewing a horizontally placed white reference panel in the nadir direction. (b) A numerical simulation of sensor readings with $d_c$ = 0 and $E_0$ = 110 units. The eastward tilted sensor is 1° from the horizontal. The sun position is computed for the same time location as in the measurement.

Fig. 7 shows the combined influence of tilt surfaces, diffuse fraction and sun zenith angle on sensor-pair calibration. For a sun zenith angle of 20°, in the case of our *in situ* calibration at African Sahel sites, the relative error in slope $k$ is less than 1.5% for any diffuse fraction if the tilt angles of the sensor pair surfaces are less than 1°, implying the *in situ* calibration in those sites is relatively easier. For a sun zenith angle of 40°, in the case of Nordic region sites, the surface tilt from the horizontal should be less than 0.5°, in order to render the relative error in $k$ less than 1.5%. For the larger solar zenith angle 60°, in the case of Arctic region sites, to ensure an error in $k$ no larger than 1.5% requires either high diffuse fraction (>0.35 if the level accuracy is 0.5°) or accurately levelled sensor surface (tilt <0.3° considering some diffuse fraction in a sky with large solar zenith angle [29, eq. (3)]), implying *in situ* calibration in those sites is relatively more difficult (including the possible deterioration by the highly reflective snow background). In order to ensure the accuracy of slope $k$, the measurement should be made either 1) under overcast sky, or 2) at around solar noon time, or 3) with accurately levelled light sensing surfaces. In the following section we will use 1.5% relative error in $k$ from tilt surface to evaluate combined uncertainties.

## C. *Uncertainty evaluation*

### *1) Reflectance uncertainty*

We used 1.2% as a standard uncertainty from repeat test, 1.5% as slope uncertainty from the numerical simulation (may be feasibly achieved), and 0.3% of the reflectance factor uncertainty of the white reference panel involved (from the calibration certificate by the manufacturer). We estimated a combined standard uncertainty in slope $k$ as 2% by (22). Therefore the standard uncertainty in reflectance measurement due to the uncertainty in user calibration was estimated as 2% from (18).

The standard uncertainty in reflectance measurement due to the uncertainty of manufacturer calibration of sensitivity parameters was estimated as 3.5% by (17), given the claimed

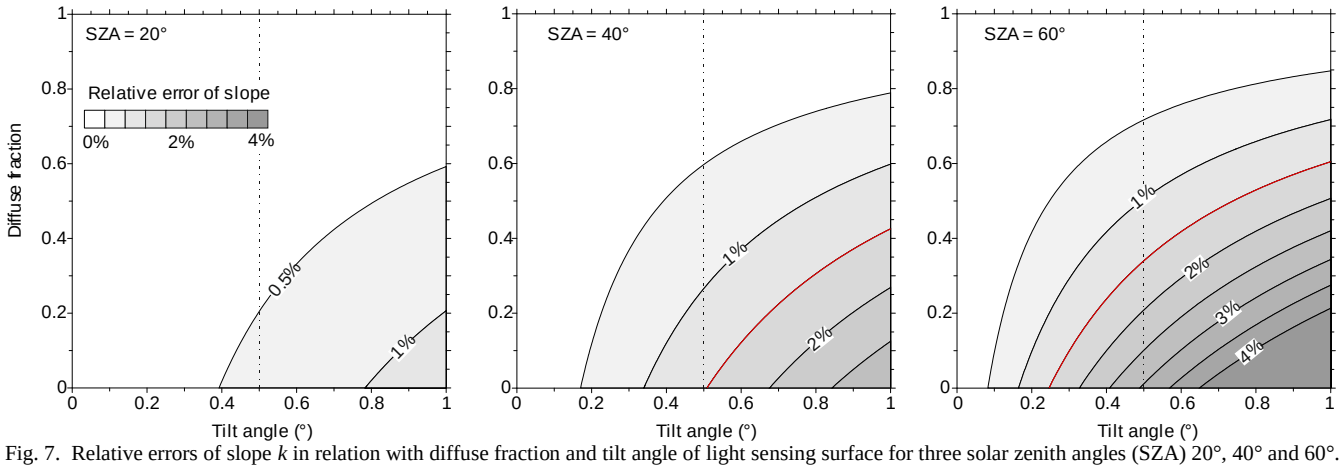


Fig. 7. Relative errors of slope $k$ in relation with diffuse fraction and tilt angle of light sensing surface for three solar zenith angles (SZA) 20°, 40° and 60°. Red isoline shows 1.5% relative error of $k$, and an error no bigger than this can be feasibly achieved during calibration by accurately levelling sensor surfaces. Dash-dot line denotes a tilt angle of 0.5°.

expanded uncertainty of 5% in sensitivity by the manufacturer.

*2) NDVI uncertainty*

Using the above standard uncertainty level in reflectance measurement, the estimated NDVI uncertainties from user calibration and manufacturer calibration for sensor pair were computed with (19) and plotted in Fig. 8(a). For the single-sensor method, the main uncertainty in slope $k_s$ was attributed to the difference of the red:NIR ratio during NDVI measurement from the ratio during calibration. Such uncertainties are exemplified by 1% difference and 10% difference in Fig. 8(b) using (20).

The plots show that NDVI measurement uncertainty decreases sharply with increasing NDVI level. Larger NDVI has smaller measurement uncertainties, whereas the smaller NDVI has larger uncertainties. The uncertainty in measured NDVI may be less than 5% for NDVI above 0.2 by user calibration on a sensor pair. However, when using calibration parameters from the manufacturer, the NDVI uncertainty may be close to 10% at an NDVI level of 0.2. For single-sensor method by user calibration, the NDVI uncertainty depends largely on how the red:NIR ratio differs from the value during calibration, as well as the NDVI level, i.e. the vegetation density. For a relatively constant red:NIR ratio with the difference less than 1% between calibration and field measurement, the NDVI uncertainty can be smaller than sensor-pair method. Therefore the single-sensor method may be used to cross-check the NDVI from sensor pair measurement, particularly if the upward-looking sensor of the sensor pair is prone to dirt and raindrop persistence or for other reasons the irradiance measurement with the sensor is suspicious. However, if the difference in the red:NIR ratio of daylight is as large as 10%, the NDVI may have large uncertainty (about 25% for an NDVI of 0.2). But for dense vegetation with an NDVI above 0.6, the NDVI uncertainty can still be less than 5%.

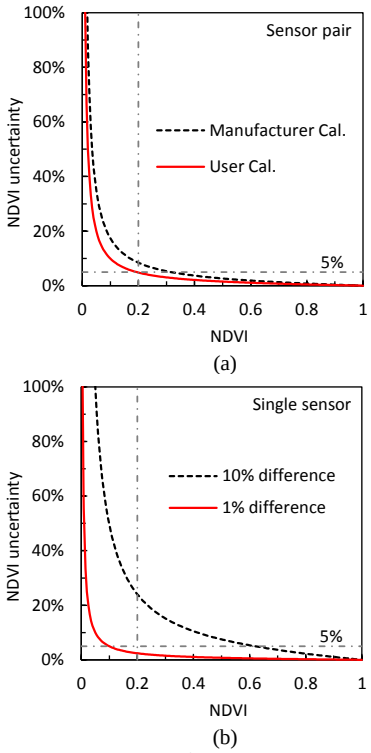


Fig. 8. NDVI uncertainties estimated from the error in sensor calibration. (a) Sensor-pair method, comparison of user calibration and manufacturer calibration. (b) Single-sensor method, comparison of the 1% and 10% differences in red: NIR ratio of daylight illumination during NDVI measurement vs. calibration.

### D. Field NDVI time series

Generally, the sensor-pair method with manufacturer calibration and *in situ* calibration produced almost consistent NDVI time series (Fig. 9), though the manufacturer calibration was 3-4 years old. Single-sensor NDVI agreed well with sensor-pair NDVI from user calibration in most days of the 2012 and 2013 growing seasons, in which the NDVI level was high (0.6~0.7). The simultaneously recoded red:NIR ratio was 1.30 ± 0.09 of all measurements at 12:00, and appeared rather noisy in Fig. 9. Single-sensor NDVI was noisier than sensor-pair NDVI, but it looks still amazingly accurate, much less noisier than the time series of red:NIR. The figure suggests that the single-sensor NDVI may be used to cross-check sensor-pair NDVI, better with clear sky measurement and preferably for dense vegetation.

## VIII. Discussion

This paper provides a systematic method of user-level *in*

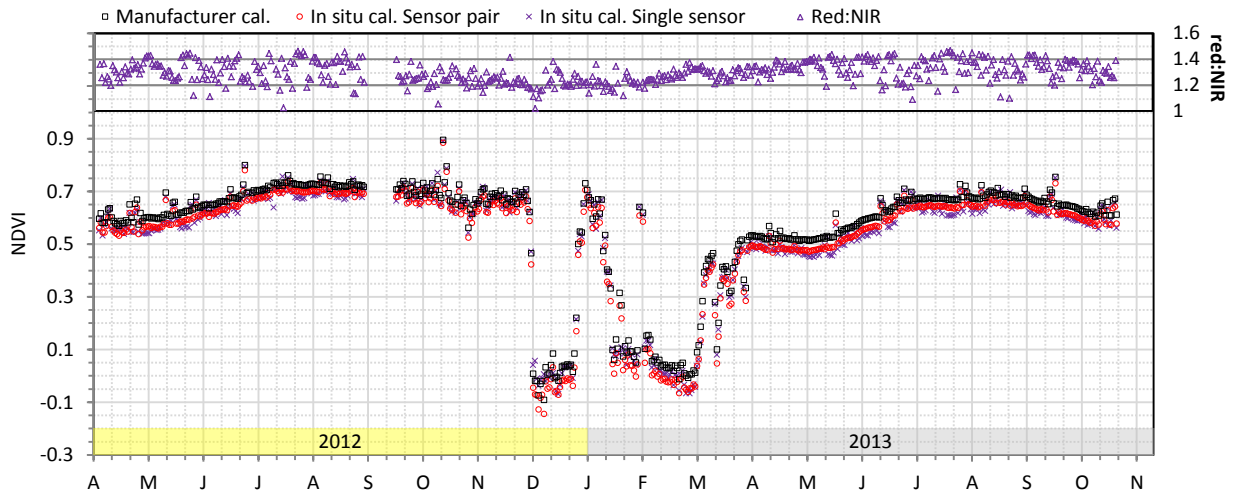


Fig. 9. Comparison of field measured NDVI from user *in situ* calibration (both sensor-pair and single-sensor methods) and manufacturer calibration over Fäjemyr peatbog, S. Sweden. The red:NIR ratio of illumination was computed from upward-looking hemispherical view sensor. The time series are daily measurements at 12:00.

*situ* calibration of light sensor pair to estimate vegetation reflectance and NDVI or other relevant spectral indices. Free daylight is used as the illumination source in calibration, enabling one to sample a large quantity of calibration data for statistical fitting analysis with high accuracy. Also, because the spectrum of artificial lights may differ substantially from solar spectrum, and therefore the laboratory calibration is insufficient for field vegetation monitoring considering the wavelength-dependent responses of the materials used in a cosine diffuser or a white reference panel. The measurement results and uncertainty analysis show that the user calibration in daylight can be as accurate as, or even more accurate than manufacturer calibration, and may guarantee more reliable long-term field spectral measurements of vegetation. The calibration method in this paper remedies the situation that reflectance for large FOV sensors (20°~60°) cannot always be estimated from manufacturer calibration due to the difficulty to make a radiometric calibration [30],[31]. The calibration of hemispherical viewing sensor pair involves no reference standard and may be viewed as an integrated pre-step for measuring absolute BHR, instead of a calibration by definition [32]. The calibration of conical-FOV sensor is against a white reference panel and the panel should be calibrated so as to facilitate comparisons of vegetation measurements cross sites and through time.

The sensor pair calibrated with this method should have light sensing surfaces with similar directional response so as to minimize the bias due to sky condition variations shown in other tests (e.g. [11],[18],[33]). Sensor pairs with identical cosine diffusers measuring albedo, like PAR sensor pairs or hemispherical-view NDVI sensor pairs, meet this requirement. If a white reference panel is used to calibrate conical-FOV sensor, the upward-looking sensor with a cosine diffuser should have a directional response similar as the white panel. A Spectralon white panel has a decreased relative response to light incident from larger angles [34],[35], which is quite similar to the light response of the acrylic diffuser [23] used on the SKR-series multispectral light sensors tested by Jin [27]. Therefore irradiance measured with a cosine diffuser is comparable to that with a Spectralon white panel, and non-Lambertian response of both materials might be negligible when computing the sensitivity ratio. The diffuse receptor of a PAR sensor usually has an enhanced response to light from larger incident angles, by allowing light incident through the diffuser edge meanwhile limited by an outer black rim [23],[36]. Its directional response is different from a Spectralon panel response (See Fig. 3). Such a PAR diffuser head design aims at obtaining a near-Lambertian response across a hemispherical view, not suitable for making cross-calibration against a white diffuse panel. Garrity *et al.* [18]'s home-made sensor adopted a similar PAR cosine-head design, while they calibrate it against a white panel. The cosine head (UNI435, PP Systems, Amesbury MA, USA) used by Gamon *et al.* [11] and the one used by Anderson *et al.* [33] are other cases similar to a PAR sensor. This explains why cloudy sky gives a larger calibration factor than cloudless sky reported by Gamon *et al.* [11], because the former sky has a higher fraction of light incident from larger angles than the latter. Given a similar directional response, the calibration slope factor $k$ in our sensor-pair method will not be affected by different sky conditions if the light sensing surface is accurately levelled during calibration.

Our calibration tests were only made on a limited number of sensors of a particular brand. Do not take the test results as sensor quality demonstration but rather an investigation of a possible *in situ* calibration method. The uncertainty evaluation in the paper was focusing on the errors propagated from calibration and should not be viewed as an uncertainty budget in vegetation reflectance and NDVI measurements, which is beyond the scope of the paper. Nevertheless, the uncertainty evaluation (19) can be used to assess how reliable the NDVI is, no matter whether the error is from calibration or other sources, like sensor tilt on the top of the mast and temperature induced drift. Fig. 8 suggests that NDVI is remarkably robust against noise in measurement, particularly for dense vegetation. The figure also provides some insight regarding the reliability of measuring the photochemical reflectance index (PRI, [37]). PRI has a similar formulation as NDVI, but with a quantity usually far less than 0.2, exacerbated by possibly high measurement noise in reflectance due to the

narrower bands (~5 nm) in PRI. Fig. 8(a) suggests that the uncertainty of PRI by sensor-pair method may be much higher than 10%, challenging researchers to obtain reliable data for inferring vegetation photosynthetic light use efficiency, and reducing calibration uncertainty of PRI sensors might be a solution.

We showed that the upward-looking sensor should be ensured level with very high accuracy during calibration. During vegetation measurement, sensor levelling is also required, but does it require the same high accuracy? No, since in vegetation measurement, a moderate tilt (max. 3°) from the horizontal gives rise to a relative error in irradiance usually less than 1% at around solar noon time if the ground reflection into the upward-looking sensor is very small and negligible. This can be demonstrated with the same numerical simulation as in Fig. 6(b). Moreover, do not take the calibration requirement of high sampling interval as the same requirement for vegetation monitoring either. Post-averaging is often used in vegetation sampling to reduce white noise.

We also proposed a method to calibrate a single sensor, and consequently estimate reflectance-derived NDVI. There are advantages of using ground-based single sensors for measuring NDVI. Soudani *et al.* [6] and Hmimina *et al.* [8] reported such successful application for vegetation phenology monitoring across various biomes. Their NDVI was computed from single-sensor measured radiance in red and NIR channels, and the sensor was calibrated against a spectroradiometer to enable measuring absolute radiometric quantity. However, radiance-derived NDVI differs from reflectance-derived NDVI, and the difference might be large depending on the spectral properties of red and NIR channels of the sensor. Satellite NDVI products are usually computed from reflectance measurement; therefore, NDVI from near-surface measured reflectance is needed to validate satellite data. We present a way to compute such single-sensor reflectance-derived NDVI with a much easier calibration, even though the actual reflectance cannot be measured by a single sensor. The shortcoming of single-sensor method is that it is not applicable for variable sky conditions. However, the single-sensor method only requires the data from the downward-looking sensor of a sensor pair, and using only clear-day observations can be a way of cross-checking NDVI from the sensor pair and avoiding some of the error associated with irradiance measurement by the upward-looking sensor, for example, dust persistence when measuring in semi-arid areas, or water stain when measuring in rainy areas.

## IX. Conclusions

We proposed a practical method for user calibration of light sensors using daylight, which gives accurate results and may contribute to improved reliability of long-term continuous vegetation monitoring. The method is suitable for calibrating multispectral or PAR sensor pairs for measuring bihemispherical reflectance (albedo) or hemispherical-conical reflectance. High calibration accuracy can be achieved if calibration procedures proposed in this paper are followed, particularly carefully levelled light sensing surfaces, neither shadows nor adjacent reflections onto the surfaces, and high data sampling rate without post-averaging. The method is not suitable for dual-view spectrometers with one near-Lambertian cosine diffuser and the other conical-FOV fore optic. A single-sensor method is proposed here as a complementary means of measuring and cross-checking dual-sensor NDVI, but it has limited use. We suggest carrying out user calibration in daylight regularly to ensure reliable and ground-based long-term multispectral measurement of vegetation.

## Acknowledgment

Thanks to our colleagues Drs. Jonas Ardö, Ford Cropley and Magnus Lund for their helps and feedbacks on the field calibration of NDVI sensors in Senegal, Sudan and Greenland. Thanks to Gareth Sims of Skye Instruments Ltd for useful discussions. We are grateful to Dr. Alasdair MacArthur of FSF, Edinburgh University for the sensor directional response test and useful discussions. The two anonymous reviewers are thanked for their constructive comments that led to a substantial improvement of the paper.

## References

[1] J. L. Monteith, "Light distribution and photosynthesis in feld crops," *Annals of Botany*, vol. 29, no. 1, pp. 17-37, January 1, 1965, 1965.

[2] G. S. Birth, and G. R. McVey, "Measuring the color of growing turf with a reflectance spectrophotometer," *Agron. J.*, vol. 60, no. 6, pp. 640-645, 1968.

[3] J. A. Gamon, A. F. Rahman, J. L. Dungan, M. Schildhauer, and K. F. Huemmrich, "Spectral Network (SpecNet)--What is it and why do we need it?," *Remote Sens. Environ.*, vol. 103, no. 3, pp. 227-235, 2006.

[4] T. Hilker, N. C. Coops, Z. Nesic, M. A. Wulder, and A. T. Black, "Instrumentation and approach for unattended year round tower based measurements of spectral reflectance," *Comput. Electron. Agric.*, vol. 56, no. 1, pp. 72-84, 2007.

[5] M. Balzarolo, K. Anderson, C. Nichol, M. Rossini, L. Vescovo, N. Arriga, G. Wohlfahrt, J.-C. Calvet, A. Carrara, S. Cerasoli, S. Cogliati, F. Daumard, L. Eklundh, J. A. Elbers, F. Evrendilek, R. N. Handcock, J. Kaduk, K. Klumpp, B. Longdoz, G. Matteucci, M. Meroni, L. Montagnani, J.-M. Ourcival, E. P. Sánchez-Cañete, J.-Y. Pontailler, R. Juszczak, B. Scholes, and M. P. Martín, "Ground-based optical measurements at European flux sites: a review of methods, instruments and current controversies," *Sensors*, vol. 11, no. 8, pp. 7954-7981, 2011.

[6] K. Soudani, G. Hmimina, N. Delpierre, J.-Y. Pontailler, M. Aubinet, D. Bonal, B. Caquet, A. de Grandcourt, B. Burban, C. Flechard, D. Guyon, A. Granier, G. P., B. Heinesch, B. Longdoz, D. Loustau, C. Moureaux, J.-M. Ourcival, S. Rambal, L. Saint André, and E. Dufrêne, "Ground-based Network of NDVI measurements for tracking temporal dynamics of canopy structure and vegetation phenology in different biomes," *Remote Sens. Environ.*, vol. 123, pp. 234-245, 2012.

[7] R. Fensholt, I. Sandholt, and M. S. Rasmussen, "Evaluation of MODIS LAI, fAPAR and the relation between fAPAR and NDVI in a semi-arid environment using in situ measurements," *Remote Sens. Environ.*, vol. 91, no. 3/4, pp. 490-507, 2004.

[8] G. Hmimina, E. Dufrêne, J. Y. Pontailler, N. Delpierre, M. Aubinet, B. Caquet, A. de Grandcourt, B. Burban, C. Flechard, A. Granier, P. Gross, B. Heinesch, B. Longdoz, C. Moureaux, J. M. Ourcival, S. Rambal, L. Saint André, and K. Soudani, "Evaluation of the potential of MODIS satellite data to predict vegetation phenology in different biomes: An investigation using ground-based NDVI measurements," *Remote Sens. Environ.*, vol. 132, no. 0, pp. 145-158, 2013.

[9] T. Tagesson, M. Mastepanov, M. P. Tamstorf, L. Eklundh, P. Schubert, A. Ekberg, C. Sigsgaard, T. R. Christensen, and L. Ström, "High-resolution satellite data reveal an increase in peak growing season gross primary production in a high-Arctic wet tundra ecosystem 1992–2008," *Int. J. Appl. Earth Obs.*, vol. 18, no. 0, pp. 407-416, 2012.

[10] L. Eklundh, H. Jin, P. Schubert, R. Guzinski, and M. Heliasz, "An

optical sensor network for vegetation phenology monitoring and satellite data calibration," *Sensors*, vol. 11, no. 8, pp. 7678-7709, 2011.
[11] J. A. Gamon, Y. Cheng, H. Claudio, L. MacKinney, and D. A. Sims, "A mobile tram system for systematic sampling of ecosystem optical properties," *Remote Sens. Environ.*, vol. 103, no. 3, pp. 246-254, 2006.
[12] T. Hilker, N. C. Coops, S. B. Coggins, M. A. Wulder, M. Brown, T. A. Black, Z. Nesic, and D. Lessard, "Detection of foliage conditions and disturbance from multi-angular high spectral resolution remote sensing," *Remote Sens. Environ.*, vol. 113, pp. 421-434, 2009.
[13] B. Pinty, and M. M. Verstraete, "GEMI: a non-linear index to monitor global vegetation from satellites," *Vegetatio*, vol. 101, no. 1, pp. 15-20, 1992/07/01, 1992.
[14] A. R. Huete, H. Q. Liu, K. Batchily, and W. van Leeuwen, "A comparison of vegetation indices over a global set of TM images for EOS-MODIS," *Remote Sens. Environ.*, vol. 59, pp. 440-451, 1997.
[15] H. Jin, and L. Eklundh, "A physically based vegetation index for improved monitoring of plant phenology," *Remote Sens. Environ.*, vol. 152, no. 0, pp. 512-525, 2014.
[16] J.-Y. Pontailler, G. J. Hymus, and B. G. Drake, "Estimation of leaf area index using ground-based remote sensed NDVI measurements: validation and comparison with two indirect techniques," *Can. J. Remote Sens.*, vol. 293, no. 3, pp. 381–387, 2003.
[17] J. Y. Pontailler, and B. Genty, "A simple red: far-red sensor using gallium arsenide phosphide detectors," *Funct. Ecol.*, vol. 10, no. 4, pp. 535-540, 1996.
[18] S. R. Garrity, L. A. Vierling, and K. Bickford, "A simple filtered photodiode instrument for continuous measurement of narrowband NDVI and PRI over vegetated canopies," *Agric. For. Meteorol.*, vol. 150, no. 3, pp. 489-496, 2010.
[19] Y. Ryu, D. D. Baldocchi, J. Verfaillie, S. Ma, M. Falk, I. Ruiz-Mercado, T. Hehn, and O. Sonnentag, "Testing the performance of a novel spectral reflectance sensor, built with light emitting diodes (LEDs), to monitor ecosystem metabolism, structure and function," *Agric. For. Meteorol.*, vol. 150, pp. 1597-1606, 2010.
[20] K. Anderson, M. Rossini, J. Pacheco-Labrador, M. Balzarolo, A. Mac Arthur, F. Fava, T. Julitta, and L. Vescovo, "Inter-comparison of hemispherical conical reflectance factors (HCRF) measured with four fibre-based spectrometers," *Opt. Express*, vol. 21, no. 1, pp. 605-617, 2013.
[21] F. E. Nicodemus, J. C. Richmond, J. J. Hsia, I. W. Ginsberg, and T. Limperis, "Geometrical Considerations and Nomenclature for Reflectance, issued by U.S. Department of Commerce, National Bureau of Standards," 1977.
[22] R. W. Thimijan, and R. D. Heins, "Photometric, Radiometric, and Quantum Light Units of. Measure: . A Review of Procedures for Interconversion," *Hortscience*, vol. 18, no. 6, pp. 818-822, 1983.
[23] W. W. Biggs, A. R. Edison, J. D. Eastin, K. W. Brown, J. W. Maranville, and M. D. Clegg, "Photosynthesis light sensor and meter," *Ecology*, vol. 52, no. 1, pp. 125-131, 1971.
[24] ISO/IEC 17025, "General requirements for the competence of testing and calibration laboratories ", ISO Committee on conformity assessment (CASCO), 2005.
[25] JCGM, "Evaluation of measurement data — Guide to the expression of uncertainty in measurement, JCGM 100: 2008," 2008, p. 120.
[26] V. Lindberg, "Uncertainties and error propagation - Part 1. In Manual on Uncertainties, Graphing, and the Vernier Caliper," Institute of Technology, Rochester, 2000.
[27] H. Jin, *Toward more reliable ground optical sampling: Multispectral sensor characteristics and traceable in situ calibrations*, http://cost-es0903.fem-environment.eu/, 2012.
[28] I. Reda, and A. Andreas, *Solar position algorithm for solar radiation applications, Technical report: NREL/TP-560-34302*, Golden, USA, 2003.
[29] F. Kasten, and A. T. Young, "Revised optical air mass tables and approximation formula," *Appl. Opt.*, vol. 28, no. 2, pp. 4735-4738, 1989.
[30] Labsphere Inc. "Technical Guide: Integrating Sphere Radiometry and Photometry," www.labsphere.com/technical/technical-guides.aspx.
[31] Y. Ohno, "NIST Measurement Services: Photometric Calibrations," *NIST Special Publication 250-37*, 1997.
[32] JCGM, "International vocabulary of metrology — Basic and general concepts and associated terms (VIM), JCGM 200: 2008," pp. 90, 2008.
[33] K. Anderson, E. J. Milton, and E. M. Rollin, "Calibration of dual-beam spectroradiometric data," *Int. J. Remote Sens.*, vol. 27, no. 5, pp. 975-986, 2006/03/01, 2006.
[34] E. M. Rollin, E. J. Milton, and D. R. Emery, "Reference panel anisotropy and diffuse radiation - some implications for field spectroscopy," *Int. J. Remote Sens.*, vol. 21, no. 15, pp. 2799-2810, 2000/01/01, 2000.
[35] T. J. Malthus, and C. J. MacLellan, "High performance fore optic accessories and tools for reflectance and radiometric measurements with the ASD FR3 spectroradiometer."
[36] J. Y. Pontailler, "A cheap quantum sensor using a gallium arsenide photodiode," *Funct. Ecol.*, vol. 4, no. 4, pp. 591-596, 1990.
[37] J. A. Gamon, L. Serrano, and J. S. Surfus, "The photochemical reflectance index: an optical indicator of photosynthetic radiation use efficiency across species, functional types, and nutrient levels," *Oecologia*, vol. 112, no. 4, pp. 492-501, 1997.

**Hongxiao Jin** received the M.E. degree in applied geophysics from Chinese Academy of Sciences, Beijing, China, in 1999, the MSc. degree in physical geography and ecosystem analysis from Lund University, Sweden in 2010.

He previously worked in engineering geophysics in a geotechnical institute under Chinese Ministry of Construction.

He is currently a PhD student studying remote sensing phenology in Lund University. He has interests in new method development, both in software and hardware for applied geosciences.

**Lars Eklundh** received the Ph.D. degree in physical geography from Lund University, Lund, Sweden in 1996.

He was with the United Nations Environment Program (UNEP) from 1989 to 1992.

He is currently Professor at Lund University. His primary research interest is remote sensing for extraction of information from land surfaces and the analysis of spatial and temporal variation of vegetation parameters.